Diabetes (db/db) Mutation-Induced Ovarian Involution: Progressive Hypercytolipidemia

DAVID R. GARRIS[1] AND BRYAN L. GARRIS

Division of Cell Biology and Biophysics, Schools of Biological Sciences and Medicine, University of Missouri-Kansas City, Kansas City, Missouri 64110

Ovarian atrophy and reproductive tract incompetence are recognized consequences of the progressive expression of the overt, diabetes-obesity syndrome (DOS) in C57BL/KsJ (db/db) mutant mice. The present studies evaluated the progressive changes in ovarian cytoarchitecture, endocrine expression, and reproductive tract cytolipidemic parameters that promote reproductive failure and ovarian involution during the pre-onset, initial, progressive, and chronic expression stages of the DOS. Paired littermate control (normal: +/?) and diabetic (mutant: db/db) C57BL/KsJ females were selected for analysis of ovarian parameters at 2 weeks (pre-onset expression of DOS), 4 weeks (initial DOS expression), 8 weeks (progressive DOS: hyperglycemic/lipidemic), and 16 weeks (overt/chronic DOS expression) of age. All 4- to 16-week-old (db/db) groups were obese, hyperglycemic, and hyperinsulinemic as compared with age-matched (+/?) controls. Prior to phenotypic expression of the DOS (2 week groups), ovarian interstitial cytolipidemia characterized the perifollicular and cortical regions of db/db tissue samples relative to +/? indices, while comparable body weight, blood glucose, as well as serum insulin and ovarian steroid hormone concentrations characterized both the +/? and db/db groups. Overt DOS expression in the 4-week-old db/db groups was characterized by body obesity, systemic hyperglycemia-hyperinsulinemia, and extensive hypercytolipidemia of ovarian folliculothecal compartments, as well as enhanced tissue lipase activities. By 8 weeks of age, progressive hypercytolipidemia characterized interstitial, thecal, and follicular granulosa cell layers of db/db tissue samples concurrent with suppressed ovarian steroid hormone production, enhanced lipid sequestration, and exacerbation of systemic hyper-glycemia/insulinemia. By 16 weeks of age, the chronic-DOS was characterized by extensive ovarian follicular involution, cortical perivascular hyperlipidemic infiltration, thecal cell atrophy, and follicular granulosa lipid imbibition. These data indicate that db/db mutation-induced ovarian structural and functional involution is a direct reflection of the cellular metabolic shift towards lipogenesis, indicated by the progressive cytoarchitectural transformation into adipocyte-like entities. The cytological indications of cellular metabolic compromise, which precede the phenotypic expression of the DOS indices, suggests that correction of these abnormal shifts in ovarian endocrine and cellular metabolism may restore, delay, or prevent the further compromise of ovarian function by db/db mutation expression. Exp Biol Med 228:1040–1050, 2003

Key words: diabetes-obesity syndrome (DOS); reproductive dysfunction; ovarian follicular atresia; (db/db) mutation; follicular hyperlipidemia; cellular lipotoxicity

Reproductive tract dysfunction is a recognized consequence of the overt expression of the diabetes-obesity syndrome (DOS) (1). In both humans (2, 3) and experimental models (4–12), utero-ovarian structural, functional, and metabolic parameters are altered in response to the progressive hyperglycemic-hyperinsulinemic systemic conditions that characterize noninsulin dependent (Type II) DOS (1, 13, 14). Suppression of cyclic ovarian follicular recruitment patterns (4, 9, 13), anovulation (12, 14), acyclicity (9, 13), depressed ovarian steroid hormone synthesis and release (16–19), hypovascularization and tissue ischemia (16–20), enhanced follicular atresia (9, 13, 16, 19), and premature tissue atrophy and involution (1) have been recognized to occur in association with overt DOS expression. Associated alterations in uterine indices, such as suppressed responsivity to ovarian steroid stimulation (1, 17, 21–23), depressed endometrial blood flow (16), limited decidualization (16), and pronounced placental-fetal growth retardation rates (3, 11, 24), have been associated consequences of DOS-induced reproductive failure. These recognized cytoatrophic and tissue involution changes have been attributed to the shift in cellular metabolism towards lipogenesis under pronounced diabetic, hyperglycemic conditions (1, 14, 17, 19, 25). The resultant lipid imbibition in affected cells and tissues suppresses the stimulated adrenergic counter-regulatory mechanisms from being effective modulators of the hyperglycemic environment (1, 25–27), promoting metabolic homeostatic imbalance, cellular adiposity, and tissue involution (1, 25). As a result of the enhanced cytolipid depositions that occur (1, 13–14), utero-ovarian tissue involution is progressively and proportionally

[1] To whom requests for reprints should be addressed at Division of Cell Biology and Biophysics, Schools of Biological Sciences and Medicine, University of Missouri–Kansas City, 5007 Rockhill Road, Kansas City, MO 64110. E-mail: garrisd@umkc.edu

Received January 29, 2003.
Accepted May 16, 2003.

1535-3702/03/2289-1040$15.00

promoted relative to the DOS-induced disruption of the structural and metabolic integrity of these tissues (9, 13, 16).

The C57BL/KsJ diabetes (db/db)-mutant mouse model demonstrates severe reproductive tract alterations following the expression of the DOS (1, 13, 14, 28). In contrast with littermate controls (+/?), the utero-ovarian tissues of db/db females exhibit a pronounced propensity towards hypercytolipidemia, characterized by massive basopolar accumulations of triglyceride- and free fatty acid-inclusions within the subnuclear regions of both endometrial epithelial tissue, as well as ovarian thecal and follicular granulosa cell compartments (1, 13, 14). The (db/db) mutants are recognized to be deficient in the long-chain leptin receptor, a factor that exacerbates the DOS complications by promoting an obese, insulin-resistant, hypertriglyceridemic endometabolic state that compromises reproductive tract cellular development, maturation, and function (16, 17, 25, 26). As the severity of the hyperglycemic-hyperinsulinemic state becomes progressively manifested with age, the rate of cellular and tissue involution in both uterine and ovarian cell types is enhanced (1). Ultimately, cellular regression and atrophic involution of the reproductive tract occurs (25). However, the initial sequence of cytological, metabolic, and endocrine parameter alterations, which characterizes these db/db-induced events, remains to be elucidated. The current studies were designed to evaluate the cellular, endocrine, and related metabolic alterations in ovarian tissue collected from genetically mutant C57BL/KsJ (db/db) mice at temporal intervals spanning pre-DOS expression of the mutation to the overt/chronic phase of the expressed DOS in this model.

Materials and Methods

Animals. Adult, female C57BL/KsJ mice (Jackson Laboratory, Bar Harbor, ME) were used in these studies. Littermate control (+/?) and diabetes-obese (db/db) genotypes were matched for phenotype, tissue sampling, blood glucose, and serum insulin concentration comparisons, serving as indices for the severity of the expressed DOS. All acyclic (13), female mice were housed, without the presence of males, 5 per cage under controlled environmental conditions (23°C), with an established photoperiod of 12 hours of light per day (lights on: 0600 hr). Blood glucose levels (Ames Glucometer method) (16), the radioimmunoassay analysis of serum insulin (Novo Industries, Denmark: 17.2 IU/mg standards) (8), radioimmunoassay of serum estradiol (E) and progesterone (P) concentrations (14), high-performance liquid chromatography (HPLC) of tissue norepinephrine (NE) concentrations (26), tissue lipoprotein and triacylglycerol lipase activities (1, 19), and body weights were monitored for each of the designated 2- (prepubertal, pre-onset stage), 4- (peripubertal, initial DOS expression stage), 8- (early adult, progressive, overt DOS stage), and 16- (adult, DOS chronic/organ regression stage)-week-old age group experimental periods as previously described (1, 25). Animals exhibiting both obesity (≥20 g by 4 weeks of age; controls ≤17 g) and pronounced hyperglycemia (≥200 mg/dl) relative to controls (≤150 mg/dl) were utilized (1, 13), with the progressive expression of these indices observed between 4 and 16 weeks of age.

Hormone Assays. Serum insulin concentrations were evaluated from duplicate pooled serum samples by radioimmunoassay (RIA) as previously described and validated (8) using mouse insulin (17.2 units/mg: Novo Industries) standards. Assay sensitivity approximated 80 pg with an intraassay variability of less than 10%. All serum insulin values were expressed as pg/ml. Serum E and P concentrations were evaluated by RIA as previously described and validated (14) from duplicate or pooled groups samples, depending on the amount of serum available. Interassay and intraassay variability approximated 10%. All E (pg/ml) and P (ng/ml) values were expressed corrected for procedural loss.

Tissue Collection and Preparation. Ovaries from 2-, 4-, 8-, and 16-week-old control (+/?) and diabetes-obese (db/db) matched-paired groups were collected, weighted, and prepared for light and transmission electron microscopic (TEM) examination as previously described (1, 13, 14). In brief, mice were anesthetized at the designated age-related experimental stages of DOS (db/db) mutation expression with sodium pentobarbital and systemically perfused with 50 ml of physiological saline and 100 ml of Karnovsky's fixative solution. Ovarian tissue samples were cleaned, blotted, blocked, and embedded in plastic using conventional techniques as previously described (13, 30) All tissue samples were subsequently sectioned and stained with toluidine blue for lipid polychromatic identification (1, 30) and localization by high-resolution light microscopic (LM) examination or with osmium tetroxide (13, 14) prior to TEM analysis.

Tissue Microscopic Analysis. Tissue sections prepared for light microscopic analysis were used for cytoplasmic polychromatic organelle designation, localization of intracellular lipid inclusion accumulations, and for the subsequent determination of cytoplasmic lipid density alterations that characterize progressive DOS cytological indices, as previously described (1, 13, 14, 19). Photographic images of ovarian interstitial, thecal, and follicular granulosa cell/tissue populations from the prepared tissue samples were captured with an Olympus (Olympus Optical, Tokyo, Japan) digital graphics camera and microscope unit, with lipid vacuole pools digitally enhanced utilizing polychromatic stain identification and digital conversion for enhanced, chemical-specific, scale imaging for analysis of cytoplasmic lipid distribution and density determinations using a computer-assisted photodigital scanner as previously described (31). All cytoplasmic lipid pool changes associated with db/db-induced, progressive cellular lipoadiposity were analyzed by high-resolution LM and digital chemospectrophotographic (DCSP) analysis as described (31) to define intercellular and intracellular lipid accumulation patterns. Tissue sections were prepared for DCSP image analysis of lipid-induced structural variations in cellular in-

tegrity, cytoplasmic changes in organelle and lipid inclusion density, as well as for translaminal and periepithelial stroma (i.e., thecal and interstitial) changes associated with the (db/db) mutation-induced cytoimbibition of interstitial lipid deposits during the designated, age-related stages of the DOS (1, 13) as previously described (31).

Tissue Norepinephrine, Lipoprotein Lipase, and Triacylglycerol Lipase Measurements. To relate the recognized DOS-induced changes in cellular and tissue structural indices to concomitant alterations in cellular metabolic status, ovarian tissue samples were collected from 2-, 4-, 8-, and 16-week-old +/? and db/db groups for analysis of noradrenergic and lipid (triacylglycerol lipase) uptake parameters. Homogenized, fresh tissue NE levels were determined by high-performance liquid chromatography (HPLC) utilizing a C-18 reverse phase uBondapak column (Waters and Associates, Milford, CA) attached to an LC-4 electrochemical detector with a carbon electrode coupled with a Ag+/AgCl reference electrode (Bioanalytical Systems, LaFayette, IN) as previously described and validated (25, 27). All NE values were expressed as nanogram per gram of fresh tissue corrected for procedural loss of the internal standard. Final calculations of tissue NE levels were performed using a Data Module 720 (Waters and Associates). Tissue lipoprotein and triacylglycerol lipase activities were measured as previously described (1, 19, 29) from triplicate pools of ovarian samples collected from 2-, 4-, 8-, and 16-week-old (+/?) and (db/db) groups. All group means (±SEM) values were expressed as nanomoles FFA/1 min/1 g tissue.

Statistical Analysis. Values for body weight, blood glucose, serum insulin levels, and tissue metabolic indices were expressed as group means (± SEM) for the designated age and genotype groups for both control (+/?) and diabetic (db/db) mice. Intergroup differences with respect to age or genotype comparisons were determined using the Student's *t*-test, Newman-Keuls, or Analysis of Variance exams, where appropriate, with a $P \leq 0.05$ accepted as representing statistical intergroup measurement differences.

Results

Temporal, Phenotypic, Metabolic, and Endocrine Indices Associated with (db/db) Expression. At 2 weeks of age (pre-DOS expression phase), the body weights, blood glucose, and serum insulin levels of both +/? and db/db groups were found to be comparable (Fig. 1). However, by 4 weeks of age (initial phase of DOS expression), the db/db groups exhibited significant increases in body weight and serum insulin concentrations relative to +/? groups, complicated by mild hyperglycemia. In contrast, by the 8-week-old, overt phase of DOS expression, all db/db indices were dramatically elevated relative to age-matched +/? parameters. These phenotypic, systemic, and endocrine indices remained elevated through the 16-week-old, organoatrophy phase of the DOS in the db/db groups relative to littermate +/? parameters (Fig. 1). In contrast, ovarian steroid hormone levels were significantly lower in db/db groups relative to +/? controls between 4 and 16 weeks of age, indexing the severity of the DOS-induced progressive suppression of follicular steroidogenic function (Fig. 2).

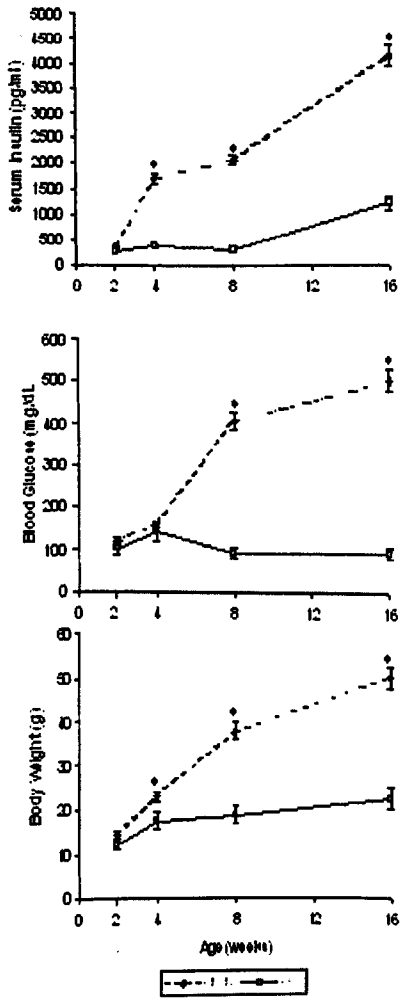

Figure 1. Age (weeks)-related changes in body weight, blood glucose, and serum insulin levels in C57BL/KsJ control (+/?) and diabetic (db/db) mice are presented as group (n = 5–8/group) means (± SEM) during the experimental period. Significant ($P \leq 0.05$) differences between (+/?) and (db/db) groups means for each respective parameter are denoted by asterisks (*).

Alterations in ovarian metabolic lipase and carboxylase activities accompanied the dramatic changes in the db/db indices during the indicated DOS phases of expression (Fig. 3). Low or nondetectable levels of lipase and carboxylase activities were observed in both +/? and db/db samples in the pre-DOS, 2-week-old groups. By 4 weeks of age, the initial expression of enhanced triacylglycerol (TG) lipase activity, an index of enhanced tissue lipid imbibition, occurred in db/db groups relative to +/?, in temporal association with the noted increase in body weight and serum insulin concentrations (Fig. 1). By 8 weeks of age, both TG and lipoprotein (LP) lipase activities were enhanced in overt-DOS phase db/db mice relative to control indices (Fig. 3). By 16 weeks of age, lipase as well as acetylCoA

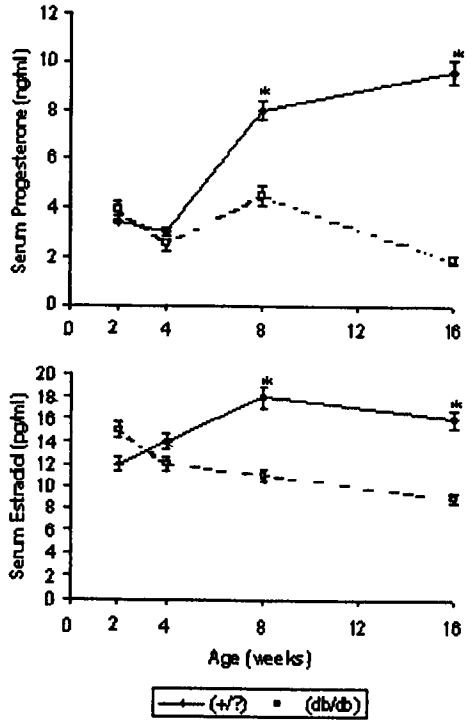

Figure 2. Age (weeks)-related changes in serum èstradiol and progesterone concentrations for control (+/?) and diabetic (db/db) C57BL/KsJ mice (n = 5–8/group) are represented as group mean values (± SEM) at specific experimental stages of the DOS. Asterisks (*) denote significant ($P \leq 0.05$) intergroup differences at the indicted DOS stage.

carboxylase activities, were dramatically elevated in db/db groups relative to littermate (+/?) controls. During the same timespan of DOS expression, the alterations in ovarian NE concentrations (Fig. 4), evaluated as an index of resulting intrinsic counter-regulatory response to db/db expression, exhibited a sharp elevation in tissue concentrations between 4 and 8 weeks of age in temporal association with the overt phase of the DOS. By 16 weeks of age, a significant decline in tissue NE accompanied the tissue involution and organoatrophy that characterized the chronic expression of the diabetes (db/db) mutation.

Ovarian Tissue and Cytological Analysis of Progressive Cytolipidemic Involution. Progressive, cellular and interstitial, ovarian involution characterized the db/db tissue samples between the 2- and 16-week-old phases of the DOS mutation expression in C57BL/KsJ mice relative to +/? groups (Fig. 5). As indicated by both LM and DCSP analysis, cytoplasmic basal pole lipid inclusions were a constant component of follicular thecal and granulosa cellular compartments, indicative of the normal cellular inclusions of triglyceride and free fatty acid pools associated with steroidal synthesis and release (Fig. 5). In +/? groups between 2 and 16 weeks of age, interstitial and follicular cell compartments demonstrated the consistent presence of cytolipid pooling (Fig. 6A,C,E,G) (Table I), which exhibited a dispersed, but constantly expanding presence in all developing and stimulated follicles exhibiting normal, non-

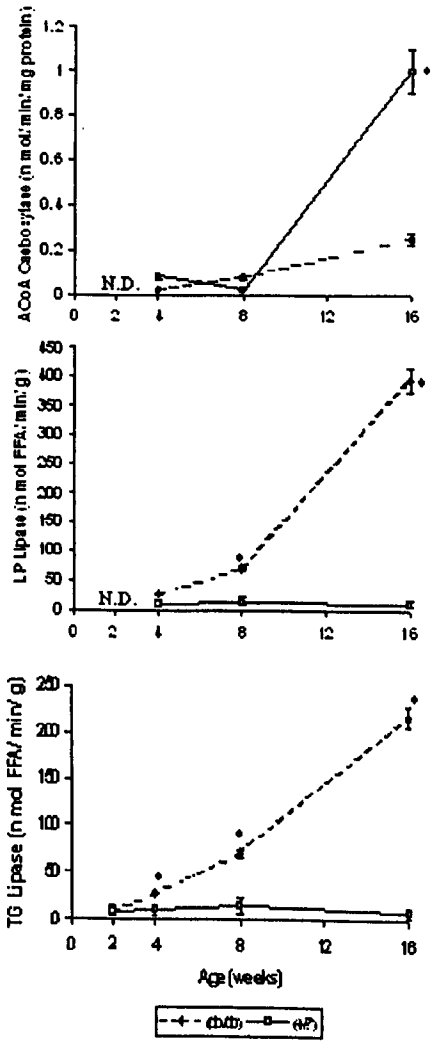

Figure 3. Age (weeks)-related changes in triacylglycerol (TG) lipase, lipoprotein (LP), lipase, and acetyl CoA (AcoA) carboxylase activities are presented as group (n = 5–8) means (± SEM) for control (+/?) and diabetic (db/db) ovarian tissue samples collected at the four designated experimental phases of mutation expression. Significant ($P \leq 0.05$) differences between group means at the designated age groups are denoted by asterisks (*).

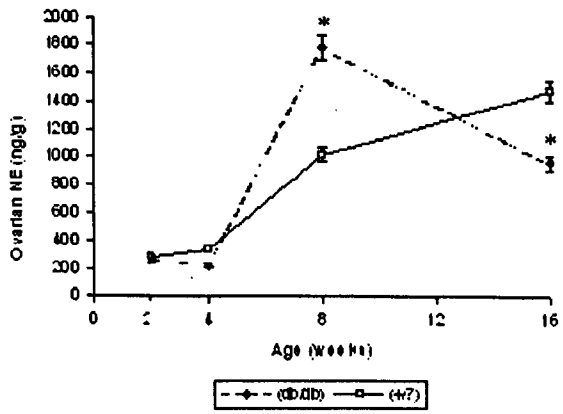

Figure 4. Alterations in ovarian norepinephrine (NE) concentrations during the age-related (weeks) experimental periods are presented as group (n = 6–10) means (± SEM). Significant ($P \leq 0.05$) intergroup differences are denoted by asterisks (*).

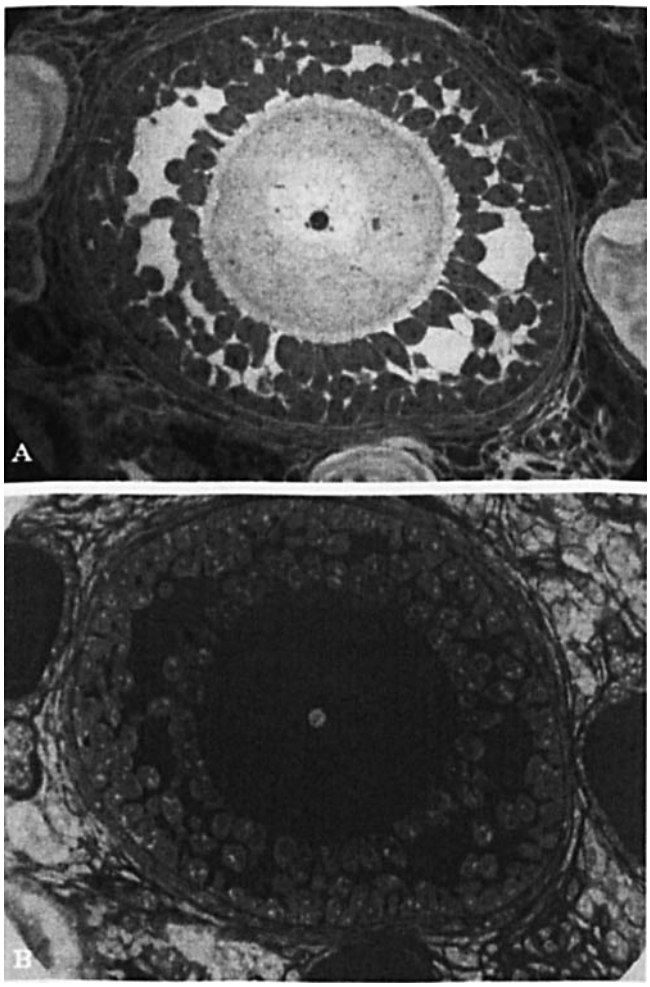

Figure 5. Photographic comparison between high resolution (×800) LM (A) and digital chemospectrophotographic (DCSP) analysis (B) of a representative ovarian antral follicle collected from a C57BL/KsJ (db/db) tissue sample at 8 weeks of age during the overt phase of the expressed diabetes mutation. By LM, interstitial perivascular lipid densities are apparent surrounding the perithecal limitations of the follicle. However, following DSCP analysis of the sample, enhanced visualization of the triacylglycerol and free fatty acids accumulations present within interstitial, thecal, and cytoplasmic granulosa loci are accentuated, as well as intercellular and intracellular trafficking patterns visibly demonstrated. The application of DCSP analysis to both control and diabetic samples collected at the four designated experimental periods of the expressed diabetes mutation was subsequently used for analysis of cytolipid toxicity and ovarian tissue and follicular involution resulting from the hyperglycemic metabolic state in this mutant model.

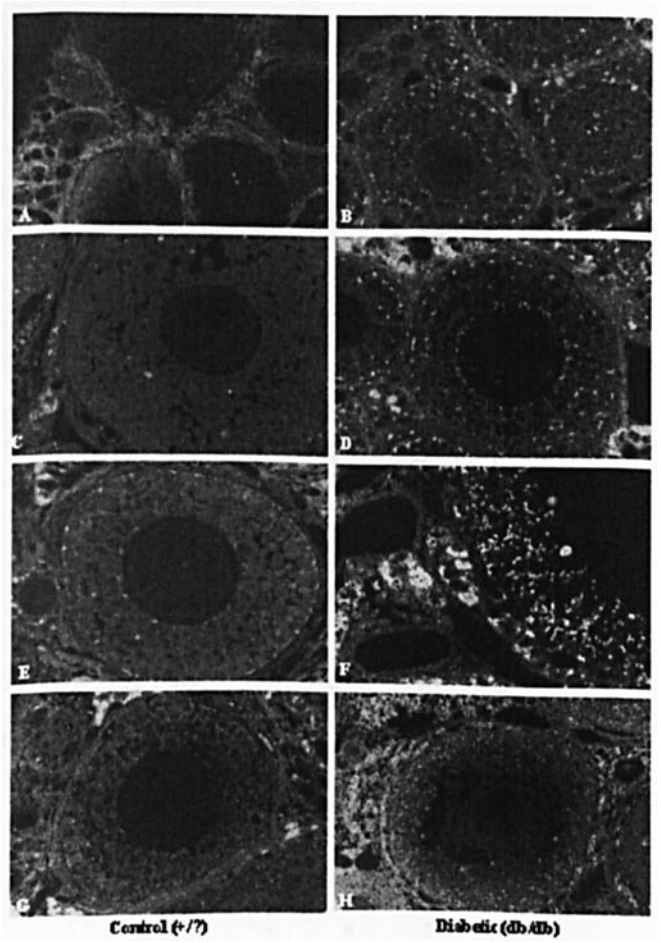

Figure 6. Representative DCSP (×800–1000) analysis of ovarian tissue samples collected at 2 weeks [(A,B) pre-mutation expression phase], 4 weeks [(C,D) initial expression phase], 8 weeks [(E,F) overt expression phase], and 16 weeks [(G,H) chronic organotrophic phase] of age from matched control (left column) and diabetic (right column) C57BL/KsJ mice. At 2 weeks of age (A,B), perivascular, interstitial, thecal, and dispersed granulose cytolipid deposits were noticeably elevated in (db/db) samples (B) relative to the low-density dispersion of interstitial lipid pools present in (+/?) tissues (A). By 4 weeks of age (C,D), the enhanced density and distribution of lipid deposits had expanded to all ovarian tissue compartments in (db/db) samples (D) relative to (+/?) samples (C). By 8 weeks of age, the uniform distribution of ovarian lipid deposition throughout the tissue compartments in (+/?) specimens was observed to be relatively uniform, whereas the density of lipid depositions was enhanced in both interstitial and follicular compartments in (db/db) samples. By 16 weeks of age (G,H), the constant distribution of low-density lipid pools in (+/?) ovarian samples (G) contrasted with the dominant elevation of compartmental lipid pools dispersed throughout all interstitial and cytoplasmic compartments of (db/db) follicles (H).

atretic, characteristics indicative of metabolic maturation and expression. Medullary perivascular, cortical interstitial, and cortical interthecal loci depositions of cytolipid pools characterized the normal ovarian tissue compartments throughout the experimental period (Figs. 6, 7A). Although the presence of cytolipid pools within the inner granulosa cell layers of developing follicles, or the presence of antral lipid vacuoles within the follicular fluid compartments of secondary follicles was rare, these sites were dominated by hypercytolipidemic accumulations in atretic follicles (Fig. 6). Thus, the localization of nominal, low-density, lipid accumulations within interstitial and follicular cellular compartments characterized all normal ovarian tissue samples during the 2- to 16-week-old experimental analysis period, and contrasted within the atresia-associated massive imbibition of intracellular lipid pools observed in C57BL/KsJ (+/?) samples (Fig. 6).

The progressive nature, influence, and severity of the db/db mutation on hypercytolipidemia-induced ovarian involution was dramatically expressed between 2 and 16

Table I. Progressive Ovarian Hypercytolipidemia: Compartmental Distribution Analysis of Diabetes-Induced Follicular Involution

Age (weeks)	Group	Control (C) or DOS phase	Ovarian compartment					
			Medullary perivascular	Cortical interstitium	Cortical interthecal	Follicular thecal	Follicular granulosa	Follicular antrum
2	(+/?)	C (Fig. 6A)	Absent	Absent	Absent	Absent	Absent	N/A
	(db/db)	Pre-DOS (Fig. 6B)	Minor accumulation	Minor accumulation	Nominal	Absent	Absent	N/A
4	(+/?)	C (Fig. 6C)	Minor accumulation	Minor accumulation	Nominal	Nominal	Nominal	Rare
	(db/db)	Onset DOS (Fig. 6D)	Present dense	Present dense	Present dispersed	Present dispersed	Present basal cells	Rare
8	(+/?)	C, (Fig. 5A;6E)	Present dispersed	Present dispersed	Present dispersed	Present dispersed	Present basal cells	Rare
	(db/db)	Overt DOS (Fig. 5B;6F;9)	Dense dominant	Dense dominant	Dense dominant	Dense dominant	Dense dispersed	Present
16	(+/?)	C (Fig. 6G;7A)	Constant dispersed	Constant dispersed	Present dispersed	Present dispersed	Present basal cells	Rare
	(db/db)	Chronic DOS (Fig. 6G;7B)	Dense dominant	Dense dominant	Dense dominant	Dense dominant	Dense dominant	Constant

weeks of age in association with the pronounced metabolic shifts towards cellular lipogenesis (Figs. 5, 6B,D,F,H). In the 2- to 4-week-old db/db groups, ovarian medullary interstitial and perivascular regions demonstrated enormous lipid depositions (Fig. 6B,D), characterized by progressive accumulations of interstitial tissue lipid pools and the presence of interthecal adipose depositions (Figs. 7B,D, 8). In addition, the prominent and persistent presence of enhanced cytolipid accumulations was a dramatic contrast with the nominal cytoplasmic lipid pool densities demonstrated by comparable +/? age groups (Table I) (Fig. 6). By the 8-week-old, overt DOS phase of the expressed (db/db) mutation, hypercytolipidemia dominated all medullary, interstitial, interfollicular, and follicular (thecal-granulosa) ovarian cellular compartments (Table I, Figs. 6, 7B,D). From LM, DCSP (Fig. 6), and TEM (Figs. 7, 8) analysis of db/db samples, all cellular cytoplasmic compartments were dominated by the enhanced interstitial lipid concentrations, inducing tissue and follicular atresia, as indexed by follicular resorption and concurrent ovarian tissue involution. The severity of the lipid imbibition resulted in the appearance of massive antral fluid depositions being detected within follicles that were succumbing to the metabolic shifts induced by the progressive expression of the (db/db) mutation (Figs. 6H, 9). Ultimately, ovarian tissue involution resulted from the massive cellular and interstitial accumulation of lipid depositions, which compromised the cytointegrity and metabolic maintenance of follicular function (Table I) (Figs. 7D, 9, 10).

Discussion

The results of the present studies demonstrate that the progressive accumulation of medullary, interstitial, and follicular triglyceride pools from ovarian perivascular compartments induced a dramatic alteration in folliculo-thecal cellular integrity, culminating in the demise of ovarian function and pronounced premature organotropy (Fig. 10). Recognized to occur in the pre-overt phase of the DOS condition, initial increases in body weight and serum insulin levels denote the first indices, which are detectable markers of the expressed (db/db) mutation, accompanied by the overt hyperglycemic state by 4 weeks of age (Fig. 1). The progressive exacerbation of these endocrine and metabolic shifts promoted the cytopathological changes, as denoted by the enhanced cellular hyperlipidemic condition and progressive loss of structural and functional integrity within the described ovarian cellular compartments of db/db groups (Fig. 10). The promotion of the DOS-associated cellular hyperlipidemia occurred in the leptin-receptor deficient (db/db) mutants under exaggerated hyperglycemic-glucotoxic indices, which are recognized to exacerbate the resultant nonregulated metabolic shift towards lipotoxicity (25–27, 31, 32). The dramatic elevations in tissue lipase activities and suppressed ovarian steroidogenesis, demonstrated that the cellular metabolic shifts towards lipogenesis were associated with the demise of cellular function. Ultimately, ovarian involution resulted from the combined actions of these indices, which induced the fatty-follicular syndrome (FFS) in db/db mutants (19), allowing for a lipid-induced demise of normal homeostatic metabolism (1, 13, 14, 17) and, progressively, the structural involution of all ovarian compartments.

The presence of cytolipid pools is a characteristic of all ovarian compartments, in both normal and DOS states, and is required to support normal endocrine steroid production responsible for the promotion of cellular maturation and metabolic stability in reproductive tract tissues (13, 15). However, the dramatic enhancement of cytolipid pools in db/db ovarian compartments serves as an index of how aggressive and progressive lipoatrophy becomes manifested

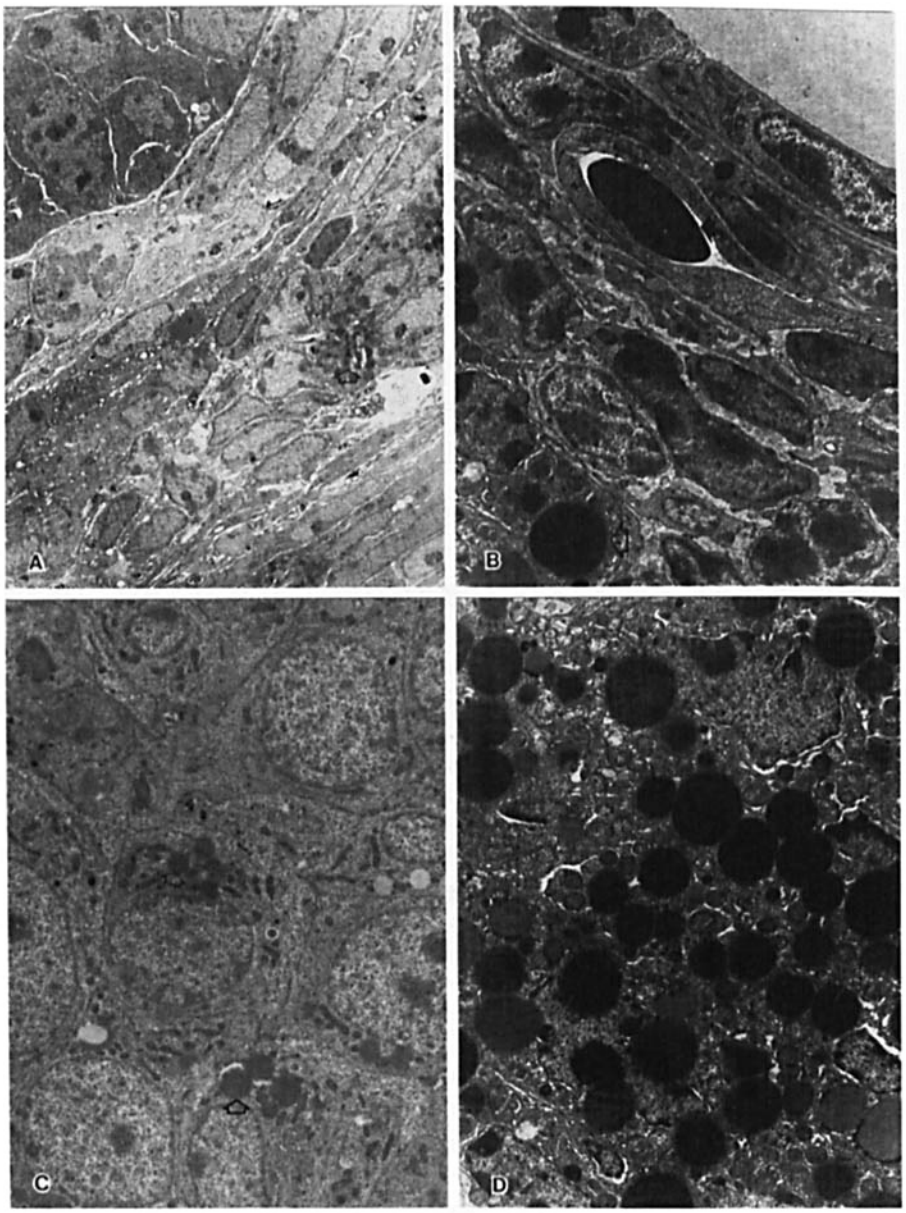

Figure 7. Contrasting TEM photographic (×7600) analysis of interfollicular regions from control (A) and diabetic (B) 4-week-old ovarian tissue samples indicate the remarkable tissue and cellular disruption that accompanies the expression of the (db/db) mutation in C57BL/KsJ mice. The isolated presence of small, localized lipid pools (open arrow) within interthecal ovarian compartments of (+/?) specimens characterized the functional maturation of these follicular loci. In contrast, the density of perivascular (closed arrow) and intracytoplasmic stromal (open arrow) lipid accumulations in (db/db) tissue (B) occurred as elevations in TG- and LP lipase activities (Fig. 3) increased under hyperglycemic-hyperinsulinemic (Fig. 1) metabolic influences. By 16 weeks of age, the granulosa cells (C) of normal follicles from (+/?) samples demonstrated the constant presence of cytoplasmic lipid pools (open arrows) dispersed within the normal organelle profile of mature cells. In contrast, granulosa cells from 16-week-old (db/db) exhibited marked cytolipid atrophy (D) and tissue involution resulting from the hyperlipidemia, which dominated the tissue profile. Although some nuclear and organelle compartments were visible in (db/db) follicles at this DOS phase, the vast majority of follicular sites demonstrated cytolipid toxicity and dissolution as a result of the chronic exposure to the existing hyperlipidemic environment.

under hyperinsulinemic-hyperglycemic conditions in the absence of leptin-mediated modulation. In the pre-expressed phase of DOS (2 weeks of age), both +/? and db/db groups demonstrated comparable lipid depositions within the interstitial, thecal, and follicular ovarian compartments. However, by the 4-week-old, DOS-onset phase of the mutation, cortical perivascular and interstitial ovarian lipid depositions were dramatically elevated in db/db mice relative to +/? littermates (Fig. 10). Associated with the initial elevation in tissue lipase activities, insulin levels, glucose concentrations, and body weight, ovarian cellular compartments were subjected to lipogenic metabolic shifts (1, 25). Instead of maintaining a maturation-associated, steroidal production of ovarian hormones, the functional decline in steroidogenesis was accompanied by the dramatic structural transformation into adipocyte-like cells (13). From elevated interstitial deposits, thecal and follicular compartment lipid pools increased dramatically (Fig. 10). In rapid succession, perithecal follicular granulosa cell compartments demonstrated enhanced lipid imbibition, which progressively migrated throughout the follicular granulosa cell layers into the antral fluid compartment (Fig. 10). Subsequently, the lipid transfer promoted the pronounced involution and atresia of the follicular population, allowing for the premature onset of organotropy (Fig. 10). Within 12 weeks of the onset of the DOS (i.e., 16-week-old db/db mice), virtually the entire ovarian follicular population exhibited cytohyperlipidemic atresia and tissue involution (Fig. 10).

It is well recognized that the noradrenergic counter-regulatory influences, as indexed by tissue norepinephrine (NE) and adrenergic receptors levels (25–27, 33, 34), are

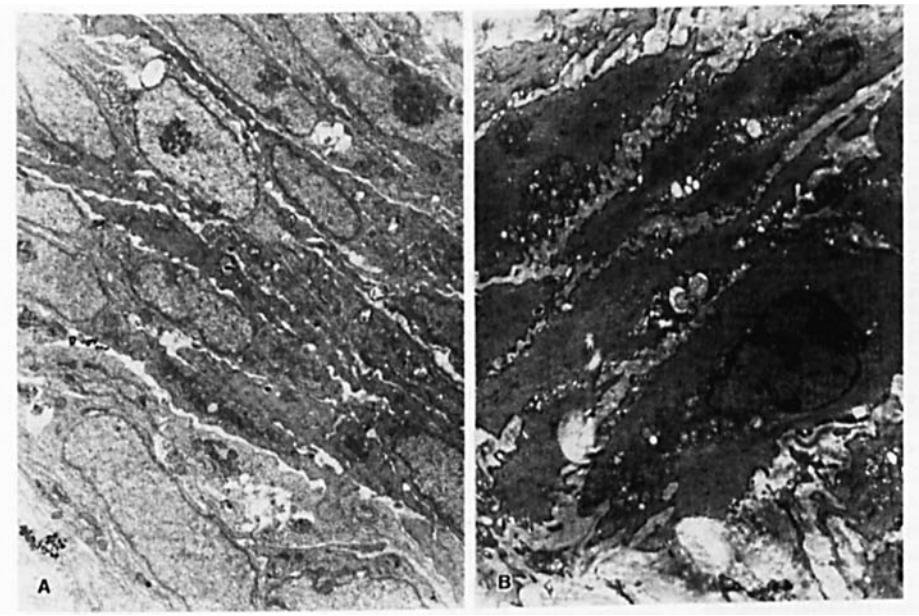

Figure 8. A dramatic contrast in the appearance and integrity of interstitial stromal cells was obvious from TEM (×10500) analysis of control (A) and diabetic (B) ovarian tissue samples collected from 8- to 16-week-old C57BL/KsJ mice. While stromal cell profiles of control samples (A) demonstrated intact and organized cytoplasmic nuclear and organelle compartments, the loss of intercellular organization and cytoplasmic organelle dissolution was characteristic of (db/db) follicular samples.

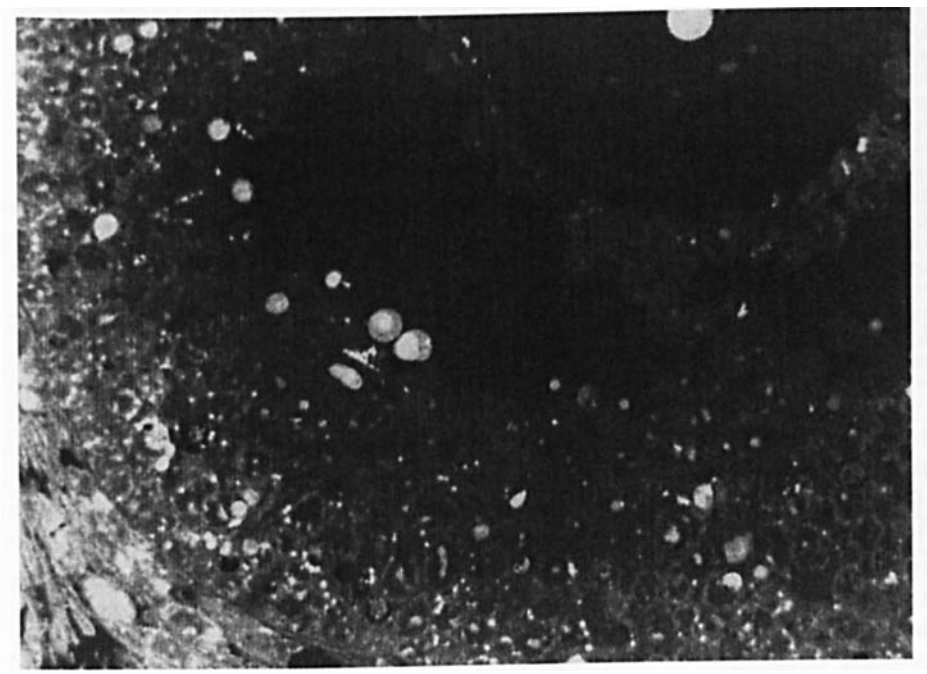

Figure 9. A high magnification (×1000) DCSP image analysis of a (db/db) antral follicle and surrounding thecal, interstitial, and perivascular ovarian tissue compartments at 8 weeks of age demonstrates the massive distribution of intercellular and intracellular lipid pools, which dominated the cellular profile following the overt expression of the (db/db) mutation. The noted trafficking patterns, which are indicated by lipid density accumulations migrating from peripheral follicular compartments into and through successive granulose layers, are distinctly visible. The eventual exocytosis of hypercytolipid granulosa pools into the antral fluids and cumulus cell clusters of follicular cores suggest the cytotoxic mechanism through which chronic expression of the (db/db) mutation ultimately induces ovarian follicular atrophy and tissue involution to become manifest under the existing hyperglycemic-hyperinsulinemic and hyperlipidemic metabolic conditions.

remarkably enhanced in response to DOS metabolic parameters in db/db mice. In addition, it is recognized that NE enhances leptin-modulated influences on fatty-acid oxidation (35). Due to the lack of intrinsic leptin receptors in the (db/db) mutants, the lipid-regulating influences of endogenous NE is compromised. Initial diabetes-stimulated elevations in tissue NE (26), α-adrenergic receptors (27), and the histofluorescent localization of NE fibers (25) all eventually succumb to the hyperlipidemic state. In db/db mice, the noradrenergic response to the insulin-resistant, hyperglycemic state becomes progressively suppressed as the lipogenic shift in ovarian metabolism compensates for the enhanced interstitial TG depositions (25). As such, with the exacerbation of the hyperlipidemic state, the expected regulatory efficacy of noradrenergic maintenance of cellular metabolism is compromised, allowing for a lipogenic dominance of cellular metabolism and the resulting induction of cellular atrophy and organ involution. The reduction of extracellular lipid depositions has been demonstrated to maintain cellular integrity in utero-ovarian tissues (1) in db/db mice and maintain noradrenergic efficacy (27). The specific mechanisms of action and effectiveness of enhanced lipid mobilization and clearance on maintaining ovarian structural and functional capacities in db/db mice is currently under investigation.

Various reports have indicated that the DOS has dra-

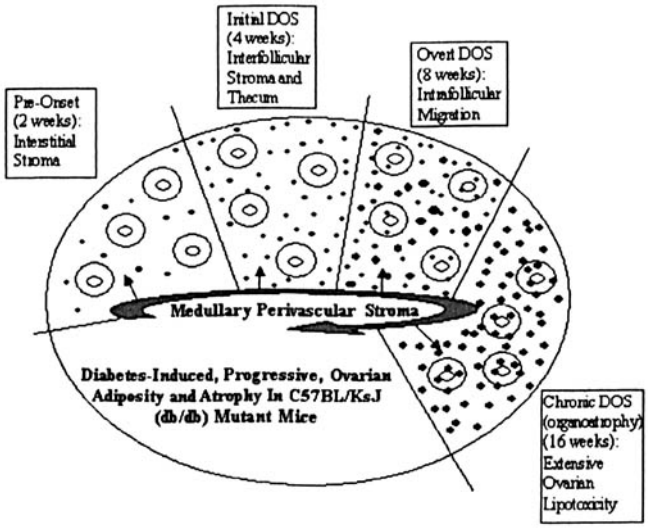

Figure 10. Graphic summary of the sequential events associated with the expression of diabetes-induced, progressive ovarian adiposity and atrophy in C57BL/KsJ (db/db) mutant mice is presented as a graphic timeline of lipid pool progression through recognized ovarian tissue compartments following the onset of the diabetes-obesity syndrome (DOS). By 2 weeks of age (i.e., pre-onset of DOS phase), the migration of circulating triglyceride-based lipid pools from the ovarian medullary perivascular stromal compartment into cortical interfollicular stromal regions has occurred. With the initial expression (4 weeks of age: initial DOS phase) of the (db/db) mutation, lipid migration and density accumulations have invaded the interfollicular stroma and perifollicular thecal layer compartments of the ovary. With the exacerbation of the systemic hyperglycemic-hyperinsulinemic metabolic state at 8 weeks of age (i.e., overt DOS phase), progressive accumulations in lipid pool densities and area expansion occupied have increased within the ovarian cortical regions, including the prominent appearance of lipid depositions and progressive migration through follicular granulosa cytoplasmic compartments. By 16 weeks of age, the chronic exposure to the DOS induced pronounced follicular and ovarian atrophic involution, promoted by the extensive cytoplasmic lipotoxicity and interstitial adiposity, which characterized C57BL/KsJ (db/db) ovarian compartments.

matic consequences on ovarian capacity to develop into functional reproductive tract tissue (1, 9, 11, 18, 28, 36). In both experimental and clinical studies, ovarian reproductive failure has been characterized by anovulation (12, 14), depressed follicular development (9, 13), suppressed ovarian steroid synthesis and release (13–16), limited corpus luteum formation and function (8), lack of uterogenic stimulation, and the incomplete support of decidua/placental formation (16). The recognized suppression of ovarian function results in the premature induction of reproductive tract tissue involution (1, 13, 14, 28). In the present studies, the uptake and deposition of lipid within the cytolipid compartments of all ovarian cell types appears to be uniquely associated with the leptin receptor defect, since previous reports using alternative models have failed to describe the apparent excessive lipo-imbibition that characterizes the tissue involution process in the db/db mutant (28). However, regardless of the exact mode by which ovarian tissue succumbs to the deleterious influences of the db/db mutation, the pronounced cyto-involution and organoatrophy are common and characteristic effects of the DOS state.

The recognized progression of hypercytolipidemia-induced organoatrophy presented in the current studies extends the recognized reproductive tract dysfunctions previously reported in both Type-I (IIDM) and other Type-II (NIDDM) experimental models (1, 8–10, 17–19) in which the causal relationships between hyperglycemia, hyperinsulinemia, and ovarian compromise have been recognized. In addition, several studies have reported similar, stage-like, progressive influences of DOS-related hypercytolipidemia on cellular structural and functional demise in pancreatic islet cells (37, 38), cardiomyocytes (39), hepatocytes (40), and other nonadipocytic cells (41) in a variety of experimental models. Although the correction of leptin-receptor deficiencies or response suppression (38, 41), as well as the effectiveness of lipolytic drugs (42), etiocholanolones (43), and ovarian steroid hormone replacement therapies (1, 22), have been reported to restore or maintain cellular and structural indices related to the obesity component of the DOS in some experimental models, specific modulation of the accompanying diabetes-related, hyperglycemia-induced, cellular complications remains to be realized. To date, neither leptin nor lipolytic drug therapies have proven to be effective in reversing the (db/db)-mutation induced changes in the female reproductive tract of the C57BL/KsJ model. When expressed on alternate genomic background strains, the expressed severity of the DOS indices in (db/db) mutants are moderated, in part due to the leptin modulating efficacy of the obesity, but not diabetes, component in these models (44). However, in metabolic situations where **both** obesity and hyperglycemia are presented during hyperlipidemic metabolic states, the severity of the cellular involution appears to be related to the induced glucotoxicity, and complicated by the progressive cytolipotoxicity (1, 8, 13, 14). This is supported by the observations that obese (ob/ob) mutation-related changes in cellular structure and function (45) may be modulated by activation of leptin-influenced cellular metabolism (45–47), but (db/db) mutation-induced cytoatrophic parameters are less responsive. Current studies focus on the therapeutic activation of alternative cellular metabolic pathways to combat the recognized hyperglycemia-induced demise of cellular function to prevent, delay, or modulate the severity of diabetes-induced cytoatrophy in reproductive tract tissues that demonstrate a severe and progressive tissue involution response to the expression of the (db/db) mutation.

In summary, the results of the present studies demonstrate that enhanced lipid deposition and cellular metabolic indices promote a very nonhomeostatic, hyperlipogenic metabolic environment within all ovarian compartments of the C57BL/KsJ (db/db) mutant relative to controls. The progressive deposition of enhanced interstitial and follicular lipid pools (Fig. 10) compromises the functional and structural characteristics of all ovarian cellular and tissue compartments, ultimately inducing a hypercytolipidemia, which contributes to premature tissue involution and ovarian failure. The efficacy of therapeutic lipolytic agents to prevent,

delay, or modify the severity of the hypercytolipidemia on ovarian competency is currently under investigation.

The authors express their sincere appreciation to Ms. Jessica Kueker for the excellent technical assistance provided during the course of these studies.

1. Garris DR. Effects of estradiol and progesterone on diabetes-associated utero-ovarian atrophy in C57BL/KsJ (db/db) mutant mice. Anat Rec **225:**310–317, 1989.
2. Hall RE, Tillman AJB. Diabetes and pregnancy. Am J Obstet Gynecol **61:**1107–1115, 1951.
3. Santonge J, Cote R. Intrauterine growth retardation and diabetic pregnancy: two types of fetal malnutrition. Am J Obstet Gynecol **146:**194–201, 1983.
4. Chieri RA, Pivetta OH, Foglia VG. Altered ovulation pattern in experimental diabetes. Fert Steril **20:**661–668, 1969.
5. Lawrence LA, Cantopoulos AN. Reproductive performance in the alloxan diabetic female rat. Acta Endocrinol **33:**175–184, 1960.
6. Davis ME, Fugo NW, Lawrence KG. Effect of alloxan diabetes on reproduction in the rat. Proc Soc Exp Biol Med **66:**638–641, 1947.
7. Sinden JA, Longwell BB. Effect of alloxan diabetes on fertility and diabetes in the rat. Proc Soc Exp Biol Med **70:**607–610, 1949.
8. Garris DR, Whitehead DS, Morgan CR. Effects of alloxan-induced diabetes on corpus luteum function in the pseudopregnant rat. Diabetes **33:**611–615, 1984.
9. Garris DR. Effects of progressive hyperglycemia on ovarian structure and function in the spontaneously diabetic Chinese hamster. Anat Rec **210:**485–489, 1984.
10. Garris DR, Williams S, Smith-West C, West L. Diabetes-associated endometrial disruption in the Chinese hamster: structural changes in relation to progressive hyperglycemia. Gynecol Obstet Invest **17:**293–300, 1984.
11. Miller HC. The effect of pregnancy complicated by alloxan diabetes on the fetuses of dogs, rabbits and rats. Endocrinology **40:**251–259, 1947.
12. Garris DR, Smith C, Davis D, Diani AR, Gerritsen G. Morphometric analysis of the hypothalamic-ovarian axis of the ketonuric-diabetic Chinese hamster: relationship to the reproductive cycle. Diabetologia **23:**275–279, 1982.
13. Garris DR, Williams SK, West L. Morphometric evaluation of the diabetes-associated ovarian atrophy in the C57BL/KsJ mouse: relationship to age and ovarian function. Anat Rec **211:**434–443, 1985.
14. Garris DR. Diabetes-associated alterations in uterine structure in the C57BL/KsJ mouse: relationship to changes in estradiol accumulation, circulating ovarian steroid levels and age. Anat Rec **211:**414–419, 1985.
15. Foreman D, Kolettis E, Garris D. Diabetes prevents the normal responses of the ovary to FSH. Endocr Res **19:**187–205, 1993.
16. Garris DR. Effects of diabetes on uterine condition, decidualization, vascularization and corpus luteum function in the pseudopregnant rat. Endocrinology **122:**665–672, 1988.
17. Garris DR, Coleman DL, Morgan CR. Age- and diabetes-related changes in tissue glucose uptake and estradiol accumulation in the C57BL/KsJ mouse. Diabetes **34:**47–52, 1985.
18. Garris DR. Depressed progesterone accumulation by the brain and peripheral tissues of diabetic C57BL/KsJ mice: normalization by estrogen therapy. Horm Res **25:**37–48, 1987.
19. Garris DR, West RL, Pekala PH. Ultrastructural and metabolic changes associated with reproductive tract atrophy and adiposity in diabetic female mice. Anat Rec **216:**359–366, 1986.
20. Nylund L, Lunell NO, Lewander R, Persson B, Sarby B. Uteroplacental blood flow in diabetic pregnancy: measurements with indium 113 nm and a computer-linked gamma camera. Am J Obstet Gynecol **144:**298–304, 1982.
21. Kirkland JL, Barrett GN, Stancel GM. Decreased cell division of the uterine luminal epithelium of diabetic rats in response to 17-*B*-estradiol. Endocrinology **109:**316–318, 1981.
22. Barlett PB, Garris DR. Estradiol and progesterone modulation of glucose uptake rates by peripheral tissues in diabetic C57BL/KsJ mice. Med Sci Res **17:**387–389, 1989.
23. Barlett PB, Garris DR. Diabetes-associated alterations in cytosolic estradiol receptor binding in the peripheral tissues of C57BL/KsJ mice. Med Sci Res **15:**1421–1422, 1987.
24. Watanabe G, Ingalls TH. Congenital malformations in the offspring of alloxan-diabetic mice. Diabetes **12:**66–72, 1963.
25. Garris DR, Garris BL. Lipotrophic diabetes-associated utero-ovarian dysfunction: influence of cellular lipid deposition on norepinephrine indices. Horm Res **58:**120–127, 2002.
26. Garris DR. Reproductive tract and pancreatic norepinephrine levels in pre- and overt-diabetic C57BL/KsJ mice: relationship to body weight, blood glucose, serum insulin and reproductive dysfunction. Proc Soc Exp Biol Med **189:**79–83, 1988.
27. Garris DR. Effects of estradiol and progesterone on reproductive tract atrophy and tissue adrenergic indices in diabetic C57BL/KsJ mice. Proc Soc Exp Biol Med **193:**39–45, 1990.
28. Johnson LM, Sidman RL. A reproductive endocrine profile in the diabetes (db) mutant mouse. Biol Reprod **20:**552–559, 1979.
29. Nilsson-Ehle P, Schotz MC. A stable radioactive substrate emulsion for assay of lipoprotein lipase. J Lipid Res **17:**536–541, 1976.
30. Hoffman EO, Flores TR, Coover J, Garrett HB. Polychrome stains for high resolution light microscopy. Lab Med **14:**779–781, 1983.
31. Garris DR, Garris BL. Diabetes-induced, progressive, endometrial involution: characterization of periluminal epithelial lipoatrophy. Diabetes **52:**51–58, 2003.
32. Poitout V, Robertson RP. Secondary *B*-cell failure in type 2 diabetes: a convergence of glucotoxicity and lipotoxicity. Endocrinology **142:**339–342, 2002.
33. Garris DR. Alterations in norepinephrine concentrations in the female reproductive tract of Type I, diabetic, pseudopregnant rats. Med Sci Res **15:**1271–1272, 1987.
34. Garris DR. Diabetes-associated changes in tissue norepinephrine levels during the time of onset of the diabetes-obesity syndrome in C57BL/KsJ mice. Med Sci Res **15:**1493–1494, 1987.
35. Garris DR. Developmental and regional changes in norepinephrine levels in diabetic C57BL/KsJ mice: effects of estradiol and progesterone. Brain Res **89:**314–319, 1995.
36. Vomachka MS, Johnson DL. Ovulation, ovarian 17 hydroxylase activity, and serum levels of luteinizing hormone, estradiol and progesterone in immature rats with diabetes mellitus induced by streptozotcin. Proc Soc Exp Biol Med **171:**207–213, 1982.
37. Shimabukuro M, Zhou YT, Levi M, Unger RH. Fatty acid-induced *B* cell apoptosis: a link between obesity and diabetes. Proc Natl Acad Sci **95:**2498–2502, 1998.
38. Unger RH, Zhou YT. Lipotoxicity of *B*-cells in obesity and in other causes of fatty acid spillover. Diabetes **50**(Suppl 1):S118–S121, 2001.
39. Zhou YT, Grayburn P, Karim A, Shimabukuro M, Higa M, Baetens D, Orci L, Unger RH. Lipotoxic heart disease in obese rats: implications for human obesity. Proc Natl Acad Sci **97:**1784–1789, 2000.
40. Marceau P, Biron S, Hould FS, Marceau S, Simard S, Thung SN, Karl JG. Liver pathology and the metabolic syndrome X in severe obesity. J Clin Endocrinol Metabol **84:**1513–1517, 1999.
41. Unger RH, Zhou YT, Orci L. Regulation of fatty acid homeostasis in cells: novel role of leptin. Proc Natl Acad Sci **96:**2327–2332, 1999.
42. Higa M, Zhou YT, Ravazzola M, Baetens D, Orci L, Unger RH.

Troglitazone prevents mitochondrial alterations, *B*-cell destruction, and diabetes in obese prediabetic rats. Proc Natl Acad Sci **96:**11513–11518, 1999.
43. Coleman DL, Leiter EH, Appleweig N. Therapeutic effects of dehydroepiandrosterone metabolites in diabetes mutant mice (C57BL/KsJ-db/db). Endocrinology **115:**239–243, 1984.
44. Garris DR, Garris BL. Genomic influence on diabetes-induced, hypercytolipidemic, utero-ovarian involution. Fed Proceed **100:**108–109, 2003.
45. Swerdloff RS, Batt RA, Bray GA. Reproductive hormonal function in the genetically obese (ob/ob) mouse. Endocrinology **98:**1359–1364, 1976.
46. Qiu J, Mounzih K, Ewart-Toland A, Chehab FF. Leptin-deficient mice backcrossed to the BALB/cj genetic background have reduced adiposity, enhanced fertility, normal body temperature and severe diabetes. Endocrinology **142:**3421–3425, 2001.
47. Mounzih K, Lu R, Chehab FF. Leptin treatment rescues sterility of genetically obese ob/ob/ males. Endocrinology **138:**1190–1193, 1997.